The performance of various palaeointensity techniques as a function of rock magnetic behaviour – A case study for La Palma

Marilyn W.L. Monster [a,b,*], Lennart V. de Groot [a], Andrew J. Biggin [c], Mark J. Dekkers [a]

[a] Paleomagnetic Laboratory Fort Hoofddijk, Department of Earth Sciences, Utrecht University, Budapestlaan 17, 3584 CD Utrecht, The Netherlands
[b] Deep Earth and Planetary Science Cluster, Faculty of Earth and Life Sciences, VU University Amsterdam, De Boelelaan 1085, 1081 HV Amsterdam, The Netherlands
[c] Geomagnetism Laboratory, School of Environmental Sciences, University of Liverpool, Oliver Lodge Labs, Oxford Street, Liverpool L69 7ZE, UK

A B S T R A C T

Three different palaeointensity methods were applied to six historical and three carbon-dated flows from the island of La Palma (Spain); in total fifteen sites were processed. The two 20th-century flows were sampled at multiple locations as their obtained directions and intensities can be compared directly to those from the International Geomagnetic Reference Field (IGRF). After determination of the declinations and inclinations of the natural remanent magnetisation (NRM) by thermal and alternating-field demagnetisation, the samples were subjected to standard rock magnetic analyses to determine their Curie and alteration temperatures. Based on these characteristics, the sites were allocated to one of four rock magnetic groups labelled L*, L, C, and H, a division primarily based on the temperature-dependent behaviour of the low-field susceptibility that has been used in studies of other volcanic edifices. Scanning electron microscope (SEM) observations revealed little oxidation and exsolution (oxidation classes I to III). Palaeointensities were determined using the classic Thellier–Thellier method (Aitken and IZZI protocols), the microwave method and the domain-state-corrected multispecimen method. Thellier–Thellier and microwave results were analysed using the ThellierTool A and B sets of selection criteria as modified by Paterson et al. (2014). Their combined success rate was around 40%. Of the eight IGRF sites, two yielded average intensities within 10% of the IGRF value. For the microwave method, three sites reproduced the IGRF intensity within 10%. In the domain-state-corrected multispecimen protocol, just one site (site 9, 1971) passed the 'ARM-test' (applied in retrospect) and showed less than 3% progressive alteration. Its multispecimen result reproduced the palaeofield within error. The other IGRF sites over- or underestimated the palaeofield by up to 50%. The seven older sites produced plausible palaeointensities, generally within a few μT of model data, and if multiple methods were successful, the results were within error of each other. For all three PI methods, it seems that sites with low Curie temperatures (<150 °C; group L*), are more likely to pass all selection criteria while substantially over- or underestimating the palaeofield. It is hypothesised that time-dependent processes after cooling of the lava would be a prime reason for this discrepancy: PI experiments with a laboratory thermoremanent magnetisation (TRM), imparted at a temperature above the site's dominant Curie temperature but below its alteration temperature, yielded the correct intensity of the laboratory-imparted TRM. When two or three methods agree to within a few μT, the obtained palaeointensity is close to the palaeofield. Multi-method consistency provides an additional palaeointensity reliability check.

© 2015 Elsevier B.V. All rights reserved.

1. Introduction

Our understanding of the short-term behaviour of the geomagnetic field is currently hampered by a lack of reliable, well-dated full-vector records of the Earth's magnetic field that are well distributed over the globe. Geomagnetic field models such as the CALS family (e.g. Korte et al., 2011) are based on both directional and intensity data of the Earth's magnetic field. However, while it is fairly straightforward to determine palaeomagnetic directions, reliable absolute intensity data are notoriously difficult to obtain.

During the past two decades, several new approaches such as the microwave method (e.g. Hill and Shaw, 1999) and the multispecimen (MSP) method (Biggin and Poidras, 2006; Dekkers

and Böhnel, 2006; Fabian and Leonhardt, 2010) have been proposed, as well as improvements on existing methods such as the IZZI protocol (e.g. Yu et al., 2004) for Thellier–Thellier palaeointensity (PI) determination (Thellier and Thellier, 1959). Therefore, our technical ability to determine a robust palaeointensity value from lavas has increased. At the same time this array of methods enables comparison of their outcome which, in principle, would offer additional criteria to assess the reliability of a palaeointensity value. When the palaeointensity methods under consideration rely on different principles, consistency of their outcome would plead for that outcome providing the correct answer within an acceptable uncertainty. This is an approach similar to that of Böhnel et al. (2009), Brown et al. (2010), and De Groot et al. (2013a).

Here we use three families of palaeointensity methods – two versions of the classic Thellier–Thellier method, the microwave method, and the MSP protocol – and apply them to historical lavas from the island of La Palma (Canary Islands, Spain). We test the consistency between the three methods and compare the results to model data. Among our sites are two 20th-century flows, whose intensity values can be compared directly to those from the International Geomagnetic Reference Field (IGRF), providing a direct check on the accuracy of the obtained PI. Well-known locations for similar field tests of palaeointensity methods are the 1955 and 1960 Kilauea flows (Yamamoto et al., 2003; Herrero-Bervera and Valet, 2009; e.g. Böhnel et al., 2011) and 20th-century Etna flows (e.g. Biggin et al., 2007; De Groot et al., 2013b).

This contribution focusses on the southern part of the island of La Palma. Three carbon-dated and six historical lava flows were sampled. The latter six were previously sampled by Soler et al. (1984) to study the palaeosecular variation (PSV) to establish a PSV curve to date recent lavas of unknown age. Their cores were drilled in an area of at least 50 m radius to be able to detect (and thereby avoid) potential local anomalies. Along these lines, a study by Valet and Soler (1999) found directional variations of up to 15° and intensity variations of up to 20% above lava flows on La Palma and Tenerife due to uneven surfaces of underlying magnetic strata distorting the local geomagnetic magnetic field.

Our sampling campaign was primarily focussed on testing various palaeointensity methods. To obtain samples with as much homogeneity as possible, cores were drilled close together while keeping an eye on avoiding spots in the vicinity of large topographic changes. For most sites, our palaeomagnetic directions do not deviate significantly from the IGRF so the influence of local anomalies is deemed to be small. The sample collection proved to behave quite variably in terms of palaeointensity success rates and the obtained estimates of the palaeofield. To shed light on this variability the samples were rock magnetically characterised in detail. With this approach, we hope to find an optimal way to deal with non-ideal samples, as is the case in many sample collections.

2. Geological setting and sampling

The Canary Islands are a chain of oceanic volcanic islands off the coast of Morocco, built by magmatic processes related to a hotspot fixed under a plate slowly progressing eastward. La Palma is made up of two main stratovolcanoes: the older (>400 ka) conical northern shield and the younger elongated Cumbre Vieja volcano at the southern part of the island, which give the island its characteristic shape (Carracedo et al., 2001).

Only historical and sub-recent ($\leqslant$3.2 ka) flows were sampled for this study; fifteen sites distributed over nine cooling units in total (Fig. 1 and Table 1). All flows originate from the Cumbre Vieja volcano. Two sampled flows were deposited during the last century, within the range of the IGRF. As these are especially important for a proper comparison between the various palaeointensity

methods applied here, they were sampled at multiple locations. The western part of the 1949 flow was sampled near the crater (site 11) and at three lower locations (sites 1, 7 and 15). The eastern part was sampled once (site 13). Site 1 is from a different phase of the eruption than the other four (Klugel et al., 1999). The 1971 flow was sampled at three locations: near the summit of Mt Teneguía (site 9) and at two locations further away from the crater (sites 4 and 8). Palaeomagnetic directions for the 1585, 1646, 1677, 1712, 1949 and 1971 flows can be compared directly to those found by Soler et al. (1984) and to various field models, such as ARCH3K.1e, CALS3K.4e, and CALS10.1b (e.g. Korte et al., 2009, 2011).

In most cases, sampling was done in fresh road cuts. Sites were sampled in the solid parts of the flow, typically 0.5–1.5 m below the top of the massive part of the flow. At each site, 12–21 cores of 3–8 cm length and 2.5 cm diameter were drilled using a petrol-powered drill. Cores were taken close together to ensure as much homogeneity as realistically possible among the samples. This sampling strategy is not ideal to obtain palaeomagnetic directions, but is necessary to meaningfully compare the results of the palaeointensity experiments. At least eight cores per site were oriented with a magnetic compass and if possible also with a sun compass. Sun compass readings generally differ less than a few degrees from magnetic compass readings, although for the sites that have strong NRMs (e.g. sites 3, 9 and 10) the difference can be up to 22°. These occasionally large differences are in agreement with the findings of Valet and Soler (1999). These deviations are linked to topographic features at the surface of the flows. We minimised this influence on our samples by generally sampling at least 1 m above the underlying flow. If the obtained directions are close to the IGRF values, no significant effect is expected.

3. Methods

Before starting with the various palaeointensity experiments it is important to categorise the samples based on their rock magnetic properties and adjust the palaeointensity experiments accordingly. Furthermore, the palaeodirections were obtained from these palaeomagnetic and rock magnetic experiments.

3.1. Palaeomagnetic and rock magnetic analyses

3.1.1. Demagnetisation of the NRM and palaeodirections

To characterise both the thermal and coercive decay behaviour samples from all sites were demagnetised both thermally and by alternating field (AF) demagnetisation. Thermal demagnetisation experiments were conducted using a 2G DC-SQUID magnetometer (dynamic range 3×10^{-12}–5×10^{-5} Am^2, sample intensities typically at the upper end of the dynamic range) and an ASC TD48-SC thermal demagnetiser (residual field < 20 nT). Three to six samples per site were demagnetised to above their maximum unblocking temperatures in thirteen temperature steps (100, 140, 180, 220, 260, 300, 340, 380, 440, 500, 530, 560 and 720 °C). Seven to sixteen specimens per site were AF demagnetised in fifteen field steps (2.5, 5, 7.5, 10, 15, 20, 25, 30, 40, 50, 60, 70, 80, 90 and 100 mT) using a robotised 2G DC-SQUID magnetometer in a static three-axis demagnetisation set-up. At the lower temperature steps, some samples were too strong for the 2G DC-SQUID magnetometer used in the thermal demagnetisation experiments, even after cutting them into half or one-third the size of standard size specimens (25 mm in diameter, 22 mm long). The thermal demagnetisation behaviour of these specimens was later derived from the zero-field steps in Thellier-style palaeointensity experiments, measured on a JR-6 spinner magnetometer.
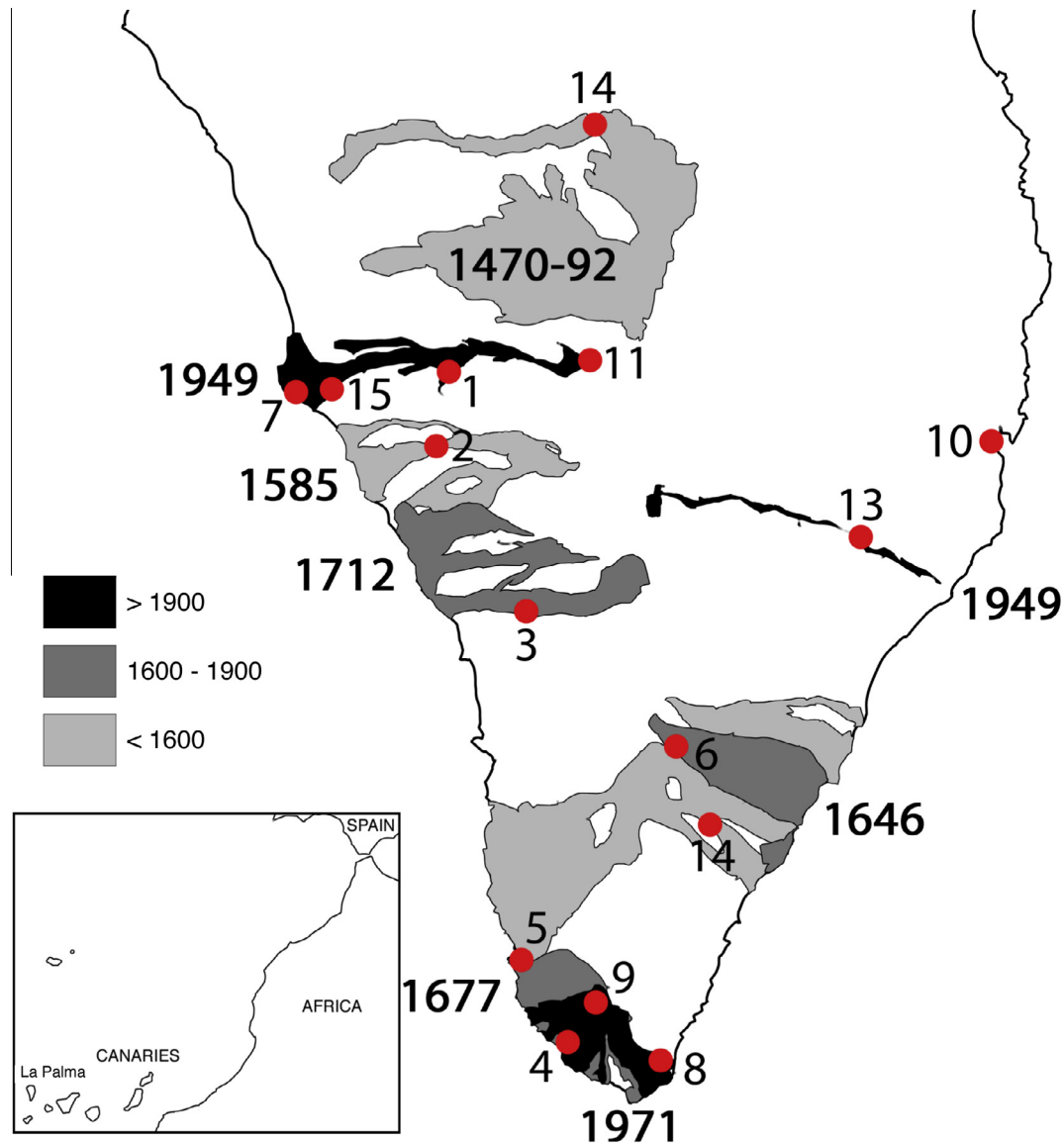
Fig. 1. Simplified geological map of the southern part of La Palma (adapted from Carracedo et al., 2001) showing the sampled lava flows. Sampling locations (for precise coordinates see Table 1) are indicated by red dots. Site numbers are shown next to the dots. The map in the inset shows the position of La Palma and the other Canary Islands with respect to Africa and Europe. (For interpretation of the references to colour in this figure legend, the reader is referred to the web version of this article.)

Palaeodirections could be obtained from both the thermal and AF demagnetisation experiments although it must be noted that the sampling routine – drilling samples as close together as possible to ensure among sample homogeneity – is not ideal to obtain reliable palaeodirections as local anomalies may not be averaged out. However, if directions compare well to the IGRF, local field anomalies are not important. The obtained directions also serve as a check to ensure that the sampled blocks are in-situ.

3.1.2. Magnetisation and susceptibility versus temperature analyses

To describe the main magnetic carriers of the samples and to determine the occurrence of alteration (albeit thermochemical or magnetic) that precludes a reliable interpretation of the palaeointensity experiments, the behaviour of the magnetisation and susceptibility of the samples was assessed as a function of temperature. In both experiments the temperature was cycled to check the reversibility of the signal; after reaching each peak temperature the temperature was lowered at least 100 °C. Curie and alteration temperatures were determined using both a modified

horizontal translation Curie balance (Mullender et al., 1993), and an AGICO KLY-3S susceptometer with a CS-3 furnace attachment (measurement frequency 976 Hz, field strength 400 A/m peak-to-peak level, noise level 2×10^{-7} SI, typical signal at least three orders of magnitude higher). The Curie balance measured the specimen's magnetisation as a function of temperature during nine temperature cycles up to 700 °C; the magnetic susceptibility was measured as a function of temperature in six cycles up to 600 °C. The 'alteration temperature' is defined here as the highest temperature reached in a thermal cycle with reversible magnetic behaviour upon cooling. At higher temperatures the magnetic behaviour of the samples is altered irreversibly, either by thermochemical alteration or transdomain processes, precluding a reliable interpretation of the palaeointensity measurements.

3.1.3. High-field rock magnetic analyses

To characterise the magnetic domain state of the flows, the saturation magnetisation M_s, the remanent saturation magnetisation M_{rs}, the coercive force B_c and coercivity of remanence B_{cr} of the

Table 1
Site locations, IGRF data, palaeomagnetic directions and rock magnetic results (T_c, T_{alt}, the viscosity index v (%), the anisotropy parameter %h (%), and finally the rock magnetic group). If a site showed multiple Curie temperatures, its secondary Curie temperature was put between brackets.

Site	UTM coordinates (zone 28R)		IGRF			Measured directions				Rock-magnetic data					
	Easting	Northing	Dec (°)	Inc (°)	Int (µT)	N (total)	α_{95} (°)	Dec (°)	Inc (°)	T_c (°C)	T_{alt} (°C)	v (%)	%h (%)	Oxidation	Group
1971 flow															
Site 4	0220339	3151984	348.0	41.9	39.1	21 (22)	2.4	349.4	35.5	540	300	2.3	2.3	II–III	H
Site 8	0222053	3151531	348.0	41.9	39.1	11 (11)	2.4	343.4	33.9	135	350	3.1	3	II	L*
Site 9	0220881	3153047	348.0	41.9	39.1	6 (10)	6.4	340.4	36.2	540	350	–	–	I	H
Combined	–	–	**348.0**	**41.9**	**39.1**	**39 (43)**	**1.7**	**347.2**	**35.5**	–	–	–	–		–
1949 flow															
Site 1	0217622	3167203	345.5	45.6	39.4	10 (10)	9.2	345.8	35.1	540	400	–	–	III	C
Site 7	0213892	3166897	345.5	45.6	39.4	9 (11)	8.1	332.6	45.1	90	300	1.7	3.2	I–II	L*
Site 11	0220775	3167210	345.5	45.6	39.4	14 (14)	1.5	342.1	49.0	80 (200)	350	–	–	I–II	L*
Site 13	0226832	3163391	345.5	45.6	39.4	14 (14)	3.0	347.0	32.2	100	350	3.2	10.1	I–II	L*
Site 15	0215216	3166630	345.5	45.6	39.4	14 (15)	2.2	351.3	45.6	90	350	2.1	1	I	L*
Combined	–	–	**345.5**	**45.6**	**39.4**	**57 (64)**	**1.9**	**345.6**	**41.0**	–	–	–	–		–
Older flows															
Site 3 (1712)	0219413	3161779	–	–	–	9 (10)	3.5	333.7	54.0	210	350	2.6	1.6	I	L
Site 5 (1677)	0219204	3153723	–	–	–	11 (11)	3.5	359.7	54.0	120	300	2.6	1.9	I	L*
Site 6 (1647)	0224141	3158590	–	–	–	12 (12)	3.1	357.5	51.6	540	300	1	2.1	I	L
Site 2 (1585)	0217376	3165247	–	–	–	11 (11)	5.3	6.4	49.0	540	350	–	–	II	C
Site 12 (1470–92)	0220737	3172548	–	–	–	11 (11)	4.3	8.2	24.1	280	325	–	–	I–II	L*
Site 10 (1.09 ka)	0229806	3165709	–	–	–	9 (10)	3.7	328.7	44.4	475	350	-	–	III	H
Site 14 (3.2 ka)	0223341	3156914	–	–	–	11 (11)	5.4	1.3	46.5	370	325	5.1	7.8	II	C

samples were measured on a Princeton Instruments alternating gradient force magnetometer (PMC Model 2900, instrumental noise level $\sim 2 \times 10^{-9}$ Am^2, typical signal at least four orders of magnitude higher). Hysteresis loops (maximum field 1 T) and back-field remanence curves were measured for three to six rock chips per flow (1–8 mg) depending on the amount of scatter among samples. The ratios M_r/M_s and B_{cr}/B_c were plotted against each other in a Day plot (Day et al., 1977) and indicate whether the grains behave magnetically 'small' (single domain (SD)) or larger (pseudo-single-domain (PSD), or multidomain (MD)).

3.1.4. Viscosity and anisotropy

To check for the presence of a viscous remanence, samples from nine sites were placed with the positive z-axis in the direction of the ambient field for a period of two weeks. After measuring the samples' remanences (M_1), they were stored in a field-free environment for an additional two weeks and measured again (M_2). The viscosity index v was determined using the definition described in Fanjat et al. (2012):

$$v = \frac{|\vec{M_1} - \vec{M_2}|}{|\vec{M_2}|} \times 100 \qquad (1)$$

Anisotropy was measured on an AGICO KLY-3 susceptometer. Its magnitude was assessed using the anisotropy parameter %h as defined by Tauxe et al. (1990):

$$\%h = 100 \cdot (\tau_1 - \tau_3) \qquad (2)$$

where the eigenvalues τ_1 and τ_3 correspond to the maximum and minimum susceptibilities.

3.1.5. Scanning electron microscopy

To visualise the degree of oxidation and exsolution, thin sections were studied with a scanning electron table top microscope (JEOL JCM-6000) in backscatter mode using 15 kV. Images were taken at various magnification factors and sites were categorised using the oxidation classes as described by Watkins and Haggerty (1968).

3.1.6. Rock magnetic groups

To adjust the palaeointensity experiments to the rock magnetic properties of the samples, all sites were placed in one of four groups based on their rock magnetic characteristics as used by De Groot et al. (2013b), following criteria defined by Calvo et al. (2002) and Biggin et al. (2007). The first group, type H, shows a distinct high Curie temperature, characterised by a constant or increasing susceptibility until at least 350 °C. The second group, type L, consists of sites with a distinct low temperature that retain less than 50% of their room temperature susceptibility at 250 °C. The third group, type C, is an intermediate group. It is either a mixture of both components or consists of magnetic minerals with intermediate Curie temperatures. Finally, type L* consists of sites that have an even lower Curie temperature than group L. Their susceptibility decreases sharply from room temperature onwards when heated, quantified by retaining less than 50% of their room temperature susceptibility at 100 °C.

3.2. Palaeointensity experiments

In most absolute palaeointensity experiments a specimen's NRM is replaced by a laboratory partial thermoremanent magnetisation (pTRM). In the classic Thellier–Thellier method (Thellier and Thellier, 1959) and its later adaptations (e.g. Coe, 1967; Aitken et al., 1988; Yu et al., 2004) the NRM is progressively replaced by a pTRM at stepwise increased temperatures in a constant known magnetic field. In multispecimen style experiments (Dekkers and Böhnel, 2006; Fabian and Leonhardt, 2010) the set temperature (i.e. the temperature at which the experiment is conducted) is kept constant throughout the experiment, but the magnitude of the magnetic field applied in the furnace is varied. It is thus possible to select a temperature for the experiment at which alteration does not occur; this temperature, however, is not always straightforward to determine, especially when transdomain processes are the reason for the alteration.

Conventionally, magnetisations are imparted in a furnace; the prolonged periods at higher temperatures, however, are known to potentially induce all kinds of alteration effects in larger PSD and MD grains (e.g. Fabian, 2001; Leonhardt et al., 2004b; Biggin, 2006; Biggin and Poidras, 2006; Draeger et al., 2006). pTRMs can

also be imparted using high-frequency microwaves of increasing power and/or duration to demagnetise and remagnetise the specimen (e.g. Hill and Shaw, 1999). The microwaves directly excite the magnetic spin system, thus reducing the heating experienced by the bulk sample and therefore the degree of alteration.

The difference between the measured palaeointensity and the expected value (for sites within the IGRF range) can be expressed as the intensity error fraction (IEF) as defined by Biggin et al. (2007):

$$IEF = \frac{PI_{measured} - PI_{expected}}{PI_{expected}} \qquad (3)$$

3.2.1. Thellier–Thellier method

In this study, two different Thellier-style protocols were used. First the Aitken protocol (Aitken et al., 1988) was used, with a laboratory field of 30 μT applied parallel to the NRM for three specimens per flow and second the IZZI protocol (e.g. Yu et al., 2004; Yu and Tauxe, 2005) was applied to up to five specimens per site with a laboratory field of 40 μT aligned in the z-axis of the samples. Numerous ways to check for thermochemical or magnetic alteration that might occur during the experiment have been proposed over the past fifty years (e.g. Coe, 1967; Aitken et al., 1988; Riisager and Riisager, 2001; Krása et al., 2003; Yu et al., 2004). We used pTRM checks (Coe, 1967) in both protocols, as well as pTRM tail checks (Riisager and Riisager, 2001) in the IZZI-style measurements.

The specimens were divided into two groups based on their Curie temperatures. The sites with lower Curie temperatures were subjected to smaller temperature steps (Aitken: 60, 80, 100, 130, 160, 200, and 240 °C; IZZI: 100 to 480 °C in steps of 40 °C) and the sites with higher Curie temperatures to larger temperature steps (Aitken: 60, 100, 145, 190, 235, and 290 °C; IZZI: 100 to 600 °C in steps of 50 °C). Generally, sites in rock magnetic group L* (see Sections 3.1.6 and 4.1.5) were placed in the first group and the other sites in the other group. It is important to note, however, that in the Aitken experiment our focus was on temperatures below the specimen's alteration temperatures and that the temperatures used in both series would normally be rather low for Thellier–Thellier-style experiments. As MD effects such as sagging will likely not be visible at these low temperatures, the obtained palaeointensities should be regarded as upper bounds of the actual palaeofield. The samples were heated in an ASC TD-48 thermal demagnetiser and all magnetisations were measured using either a 2G DC-SQUID magnetometer ('weak' samples) or a JR-6 spinner magnetometer (strong samples).

Thellier–Thellier results were analysed using the ThellierTool software (Leonhardt et al., 2004a), and the included A and B sets of selection criteria (TTA and TTB, respectively) as modified by Paterson et al. (2014). These criteria are outlined in Table 2. The selection criteria set boundaries for the following parameters that can be calculated from the Thellier results: the number of points included in the linear fit (N); the fraction of the NRM lost (f); the standard deviation divided by the slope of the fit (ß); the quality factor (q); the angular difference between the anchored and non-anchored solution (α); the anchored mean angular deviation

(MAD$_{anc}$); the relative check error (δCK) and the cumulative check difference (δpal); and (if applicable) the relative intensity difference between the original step and the tail check (δTR) and the normalised tail of pTRM (δt*) (see also e.g. Biggin et al., 2007). If more than one sample per site passed one or both sets of criteria, an additional requirement was imposed: the standard deviation divided by the obtained average palaeointensity (σ_B/B) should be less than 25%. All results failing these criteria were discarded; results that did pass the criteria but showed clear sagging or overprints are considered suspect.

3.2.2. Microwave experiments

The microwave experiments (e.g. Hill and Shaw, 1999) only differ from thermal Thellier-style experiments in the technique used to demagnetise and remagnetise the samples. By directly exciting the magnetic spin system of the remanence-carrying grains using microwaves the amount of thermal energy exposed to the sample is greatly reduced compared to conventional thermal Thellier techniques (Hill and Shaw, 1999). The various protocols and tests used in the classic Thellier–Thellier method can therefore also be used in microwave-Thellier experiments. All measurements were conducted on the microwave system installed in the geomagnetic laboratory of the University of Liverpool (UK). As each specimen was processed separately, multiple methods and laboratory fields were tested and used. Test runs indicated that the Aitken protocol using a magnetic field of 25 μT yielded the best results. The majority of the samples were therefore measured using that particular protocol. A total of 67 specimens were measured using the microwave method. Because of limited measurement time on the microwave system, the eight sites in the IGRF range were given priority. The frequency, power and duration of the microwaves were selected per sample based on its resonance frequency and its microwave NRM decay curve. e.g., for a site from rock magnetic group L* (site 11) a duration of 5 s and an increase of 1 W or less per step was used, whereas for a site from rock magnetic group H (site 9) the power was increased by 5 W per step.

In the microwave experiment some samples (in particular numerous samples from rock magnetic group L*) lost up to 50% of their NRM in an initial step merely used to test for possible changes in the sample caused by the frequency sweep used in the microwave experiment (1 W for 0.1 s, a power at which no significant change of direction or loss of NRM is expected), while their declination and inclination stayed the same. Specimens with suspicious 1 W, 0.1 s steps (i.e. more than a few per cent loss of NRM) were not taken into account when calculating average palaeointensities although their Arai plots may be interpreted. If for one specimen multiple fits passed the criteria, the one with the highest quality factor q was chosen. All data were analysed using ThellierTool 4.0 and the ThellierTool A and B sets of selection criteria (Leonhardt et al., 2004a) as modified by Paterson et al. (2014).

3.2.3. Multispecimen protocol

In 2006 the multispecimen palaeointensity experiment was proposed by Dekkers and Böhnel. Instead of using one laboratory field and multiple temperature steps, this protocol uses one temperature and multiple field levels. The DC field for which the

Table 2

Selection criteria: ThellierTool A and B (Leonhardt et al., 2004) as modified by Paterson et al. (2014). N is the number of points included in the linear fit, ß the standard deviation divided by the slope of the fit, f the fraction of the NRM lost, q the quality factor, MAD$_{anc}$ the anchored mean angular deviation, α the angular difference between the anchored and the non-anchored solution, δCK the relative check error, δpal the cumulative check difference, δTR the tail check and δt* the normalised tail of pTRM (if applicable).

	N	f	β	q	MAD$_{anc}$	α	δCK	δpal	δTR	δt*
ThellierTool A	⩾5	⩾0.35	⩽0.1	⩾5	⩽6	⩽15	⩽7	⩽10	⩽10	⩽9
ThellierTool B	⩾5	⩾0.35	⩽0.15	⩾0	⩽15	⩽15	⩽9	⩽18	⩽20	⩽99

pTRM is equal to the sample's NRM is considered to be the palae-ofield. An advantage of this method over Thellier-style experiments is that multiple specimens from the same cooling unit can be used, greatly reducing the number of heating steps and therefore possible bias due to the magnetic treatment history of the samples. Inhomogeneity may, however, induce scatter.

In the original multispecimen protocol (MSP-DB; Dekkers and Böhnel, 2006) each sample is heated only once in a laboratory field parallel to the specimen's NRM (m_1; m_0 is the NRM). Fabian and Leonhardt (2010) showed that the original claim of domain state independence (Dekkers and Böhnel, 2006) is not entirely correct and proposed two additional steps (m_2 and m_3) to quantify and correct for tail- and potential domain-state effects as well as correcting for within-site differences in the fraction of NRM lost, which may cause scatter in the MSP-DB plot. A third additional step (m_4) is a repetition of the first step, and checks for the occurrence of thermochemical or magnetic alteration that hampers a truthful interpretation of the obtained results. This protocol (MSP-DSC, where DSC is short for 'domain-state-corrected') was applied to all fifteen sites. The set temperatures for the experiments were decided based on the sites' Curie and alteration temperatures and their thermal NRM decay curves: thermochemical or magnetic alteration should be avoided, while unblocking a larger portion of the NRM during the experiment leads to a steeper slope of the linear fit and therefore a narrower uncertainty interval. For sites of rock magnetic type C and H and some sites of type L, an MSP temperature of 200 °C was used (sites 1, 2, 4, 6, 9, 10, 12, 13 and 14). For sites of rock magnetic type L* and the remainder of type L sites (sites 3, 5, 7, 8, 11 and 15) the experiment was carried out at 100 °C. The samples were heated in an ASC TD-48 thermal demagnetiser. Magnetisations were measured on a JR-6 spinner magnetometer or a 2G DC-SQUID magnetometer.

The ARM test (De Groot et al., 2012) can be used to assess whether a sample's ability to gain an ARM changes after heating to the MSP temperature. It was shown that specimens that acquire more ARM after having been heated yielded underestimates of the palaeofield in the MSP protocol. However, as the ARM test had not been developed yet when the MSP experiments in the present study were carried out, the ARM test was performed retrospectively. The single-core protocol (De Groot et al., 2012) was applied, but because generally very little material was left, for many sites the single-core experiment was not conducted with multiple specimens from the same core, but with half or quarter specimens. In the case of sites 9, 10, and 11, only very thin samples (<10 mm) were left, making exact alignment of the quarter specimens difficult. These results are therefore considered less reliable. At least eight samples (four pristine and four heated) were used per site. All ARM test measurements were conducted using the robotised 2G DC SQUID magnetometer set-up.

MSP data were analysed using a custom-made VBA macro in Microsoft Excel that calculates the Q_{DB} and Q_{DSC} ratios (the normalised differences between the remanence after the first heating step and the NRM, where Q_{DSC} is corrected for domain state effects and the fraction NRM) that are used to plot the data for the MSP-DB and MSP-DSC protocol, respectively. A number of other parameters proposed by Fabian and Leonhardt (2010) are calculated as well. Data points outside two standard error envelopes were discarded and the analysis was re-run excluding these data points. Results for sites with an average relative alteration error (ε_{alt}) (Fabian and Leonhardt, 2010) >3% are considered suspect as this implies progressive alteration or alignment issues during the experiment (De Groot et al., 2013a). Our definition of the alteration error is slightly different to that used by Fabian and Leonhardt (2010) as we do not take the absolute value in order to be able to distinguish between Gaussian errors (averaging to zero) and systematic errors (not necessarily averaging to zero).

4. Results

4.1. Rock magnetic analyses

The rock magnetic analyses presented here are used to categorise our sites based on their rock magnetic characteristics. Examples of results obtained for four typical examples (one per rock magnetic group) are included in this article itself; those of all sites can be found in Supplementary information.

4.1.1. Demagnetisation of the NRM and palaeodirections

All samples collected for this study are magnetically strong; standard size specimens generally have magnetisations beyond the dynamic range of the 2G DC SQUID magnetometer and had to be cut in half. Thermal demagnetisation behaviour shows considerable variation between the sites; the specific magnetisation per sample also varies among samples from the same site (Fig. 2, first column). Site 11, for example demagnetises very quickly, having lost most of its magnetisation at 100 °C, whereas most other sites show a much more gradual decay and site 10 even retains more than 80% of its magnetisation until 350 °C. Site 7 (1949) shows a partial self-reversal (Appendix 1), likely caused by alteration, as its AF Zijderveld and NRM decay plots do not show this reversal. At 540 °C the magnetisation of all samples was completely unblocked. Generally, specimens are AF demagnetised down to 5–20% of their starting NRM at 100 mT, with the exception of sites 9 and 12, whose samples retain up to 40% of their NRM. Zijderveld diagrams show univectorial behaviour (Fig. 2, second column) with occasionally small overprints that were removed by 5 mT or 100–140 °C. Directions obtained from AF and thermal demagnetisation appear to be consistent as are the 'within-site' NRM decay curves. Palaeomagnetic directions for the two twentieth-century flows are on average consistent with the values from the IGRF, although the directions for some sites deviate substantially – particularly the inclinations may deviate up to ten degrees for some sites (Table 1). The obtained declinations for sites 3 (1712) and 6 (1646) differ by nearly 20° and almost 10° from those found by Valet and Soler (1999) the other declinations and inclinations are consistent. For the 1712 flow, Soler and Valet (1999)'s directions are closer to model data; for the 1646 flow our data are more consistent. In the case of site 9 (1971) sun compass readings could only be obtained for four cores, significantly contributing to the scatter observed for that site (α_{95} = 6.4°).

4.1.2. Magnetisation-versus-temperature and susceptibility-versus-temperature analyses

The rock magnetic variations observed in the demagnetising spectra can also be seen in the magnetisation-versus-temperature and susceptibility-versus-temperatures diagrams (Fig. 2, third and fourth columns respectively). Sites that have low unblocking temperatures (e.g. site 11) exhibit low Curie temperatures often with a Hopkinson peak below room temperature. Curie temperatures were most easily obtained from magnetisation-versus-temperature diagrams, whereas thermochemical alteration was usually best visible in the susceptibility-versus-temperature plots. All sites appear to have alteration temperatures between 225 and 350 °C; Curie temperatures vary between 80 °C and 540 °C (Table 1).

4.1.3. High-field rock magnetic analyses

Hysteresis parameters reveal pseudo-single-domain behaviour for all sites (Fig. 3; hysteresis loops are in Appendix 1 in Supplementary information). The M_{rs}/M_s-ratios range from ∼0.06 to ∼0.3; the B_{cr}/B_c-ratios from ∼1.8 to ∼4.4. All sites except sites 11 and 12 plot on or close to the SD + MD mixing lines (Dunlop, 2002). Of these, sites 7 and 9 plot closest to the SD range, whereas
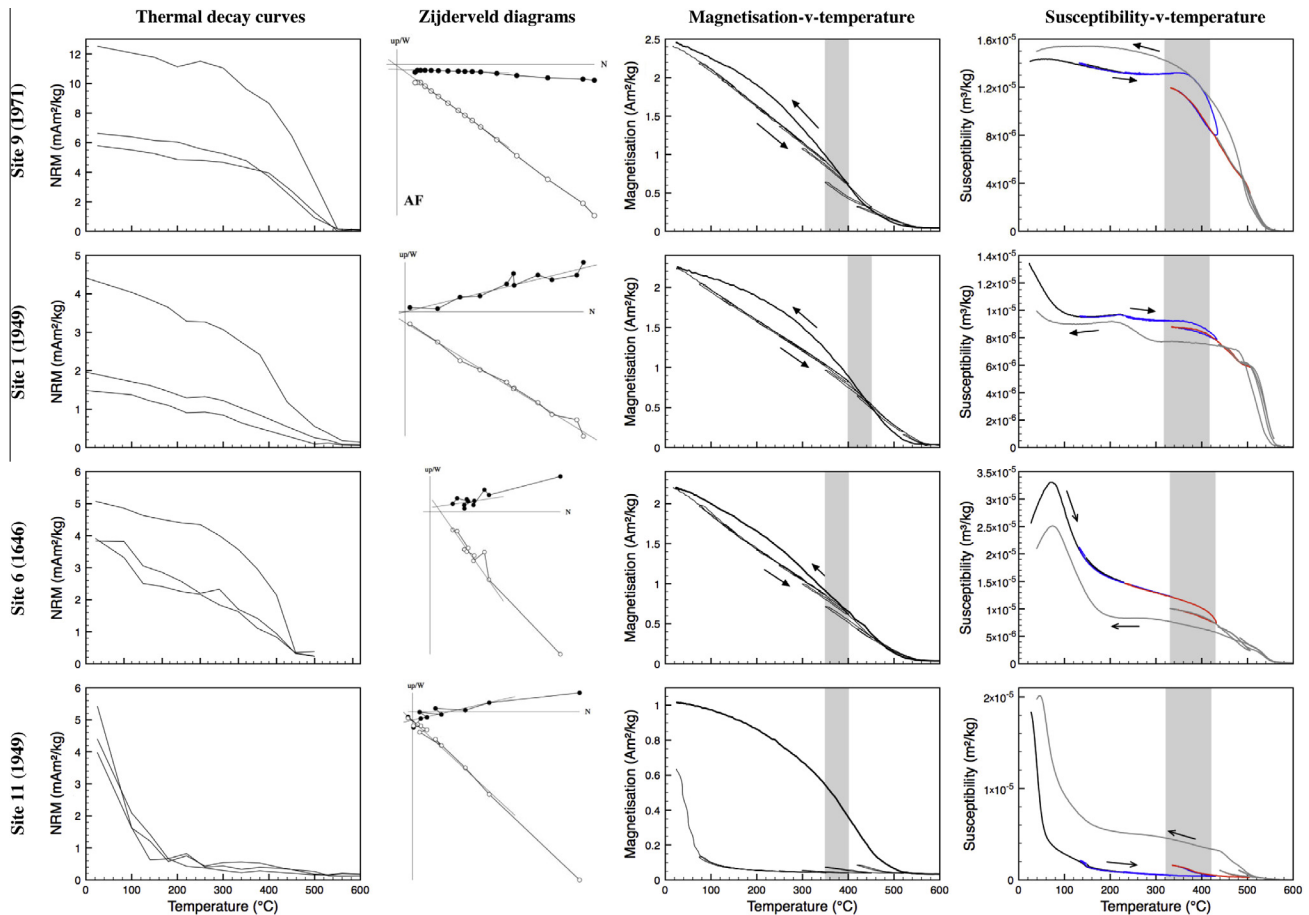
Fig. 2. Typical rock magnetic results for the four groups discerned: site 9 (1971, group H), site 1 (1949, group C), site 6 (1646, group L) and site 11 (1949, group L*). See the main text for description of group characteristics. From left to right: decay curve of thermally demagnetised NRM (100, 140, 180, 220, 260, 300, 340, 380, 440, 500, 530, 560 and 720 °C), Zijderveld diagram, magnetisation-versus-temperature plot and susceptibility-versus-temperature plot. The grey shaded areas in the latter two indicate the range in which the first alteration occurred. NRM decay curves for sites 9 and 6 were obtained from the zero field steps in IZZI-Thellier experiments (steps of 50 °C, from 100 °C to 600 °C), which were measured on a spinner magnetometer. The thermal demagnetisation was measured on a SQUID magnetometer that went out of range during the first temperature steps for most of these samples; samples shown evidently stayed within range. For site 9 an AF Zijderveld diagram is shown, as all three thermal demagnetisation specimens were initially too magnetic for the SQUID magnetometer. The robotised SQUID magnetometer used for AF demagnetisation can handle smaller specimens.
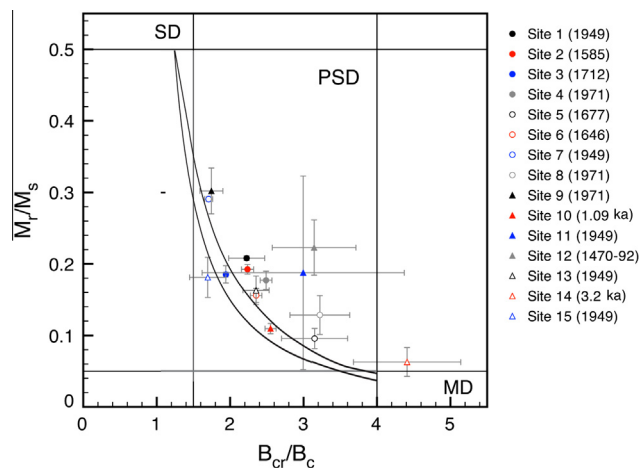

Fig. 3. Day plot for all sites including standard deviations. Three rock chips were measured per site. If the standard deviation was large ($\sigma_M > 0.03$ for M_{rs}/M_s; $\sigma_B > 0.2$ for B_{cr}/B_c), three additional chips were measured (sites 1, 5, 8, 9, 11, 12 and 14). Those sites appeared to be more heterogeneous as the standard deviations remained higher despite doubling of the data entries. Day plots per site are shown in Appendix 1.

site 14 is distinctly more MD than all others. The values of the hysteresis parameters sometimes vary significantly within a single site, as illustrated by the large standard deviation of for example site 11. As the MicroMag instrument uses very small samples (1–10 mg), this is likely related to small-scale sample heterogeneity (cf. site 11's SEM images). Day plots for individual sites can be found in the electronic supplement.

4.1.4. Anisotropy and viscosity

Most specimens (six out of nine measured sites) showed values of the viscosity parameter v (e.g. Fanjat et al., 2012) below 3% (see Table 1). Sites 8 (1971) and 13 (1949) had viscosity indices of 3.1% and 3.2%, respectively, whereas site 14 (3.2 ± 0.01 ka) had a v of 5.1%. Similarly, the degree of anisotropy %h (Tauxe et al., 1990) was generally below 3%, with the exception of sites 13 (10.1%) and 14 (7.8%). The viscosity and the degree of anisotropy therefore appear to be modest and should not have an appreciable influence on our palaeointensity experiments, except perhaps for sites 8, 13 and 14.

4.1.5. Rock magnetic groups

Based on the results from the rock magnetic analyses presented above, the various sites were categorised as one of four types using the susceptibility curves for distinction. Sites 4, 9, and 10 exhibit

high Curie temperatures and were therefore placed in group H. Sites 3 and 6 retain less than 50% of their room-temperature susceptibility at 250 °C and were therefore categorised as type L, while samples from sites 5, 7, 8, 11, 12, 13 and 15, are characterised by an even lower Curie temperature and were therefore put in group L*. The remaining sites 1, 2 and 14 are of the intermediate type C.

4.1.6. SEM

Representative SEM images are shown in Fig. 4; SEM photographs for all sites can be found in Appendix 6. Most sites revealed little to no oxidation or exsolution (see Table 1). Only sites 1 (1949) and 10 (1.09 ± 0.05 ka) showed abundant ilmenite lamellae and were therefore categorised as oxidation class III (Watkins and Haggerty, 1968). Grain size – as expected from the Day plot – varied. Site 9 (1971), which plots close to the SD range, shows mostly small grains, whereas site 14 (3.2 ± 0.01 ka), which plots in the MD range, shows only large grains. Other sites, such as 6 (1646) showed a mixture of large and small grains. Dendrite-like white 'smudges' were observed in several sites. Site 11 (1949), interestingly, revealed two distinct 'volume phases': one with few magnetite grains which were also quite large, and one with abundant small grains. This inhomogeneity also emerges in the Day plot (Fig. 3) as a large standard deviation.

4.2. Palaeointensities

4.2.1. Thellier–Thellier method

It must first be noted that as our samples are not single-domain and do show alteration (Sections 4.1.2 and 4.1.3), they – like most natural rocks – do not fulfil the theoretical requirements for Thellier–Thellier experiments. Arai plots for the four rock magnetic groups are shown in Fig. 5 and average palaeointensities per site are listed in Table 3. A full list of parameters for all samples that passed either ThellierTool A or B for one or more possible fits can be found in Appendix 2a; Arai plots are shown in Appendix 2b. As our focus in the Aitken-type experiment was on temperatures below the specimen's alteration temperature, many specimens did not pass either ThellierTool A or B because the fraction of unblocked NRM was too small. Only sites 8 (1971), 11, 13 and 15 (all 1949) yielded one or more successful results. The IZZI protocol was more successful. The average success rate for both protocols averaged over all sites was 36%.

However, when assessing the results of the Thellier–Thellier experiments it is important to distinguish between 'technically successful' (i.e. passing the selection criteria) and 'correct' (i.e. reproducing the known palaeofield within error) results. For the 1971 flow, out of the 13 specimens that passed either ThellierTool A or B (of a total of 26), only 2 samples from site 8 reproduced the actual palaeofield within 10%, and while the average of site 9 reproduces the palaeofield within 2%, neither of its two specimens that passed ThellierTool A or B were within 10% of the field. The only sample from site 9 that did reproduce the palaeofield (sample 9-2c, see the Arai plot in Appendix 2b) unfortunately did not pass either ThellierTool A or B due to one faulty check, while its Arai plot was otherwise a nearly perfect straight line. Similarly, of the 10 (out of 26) samples measured for the 1949 flow, only four specimens from site 15 reproduced the palaeofield to within 10%, whereas sites 7, 11 and 13 yielded large
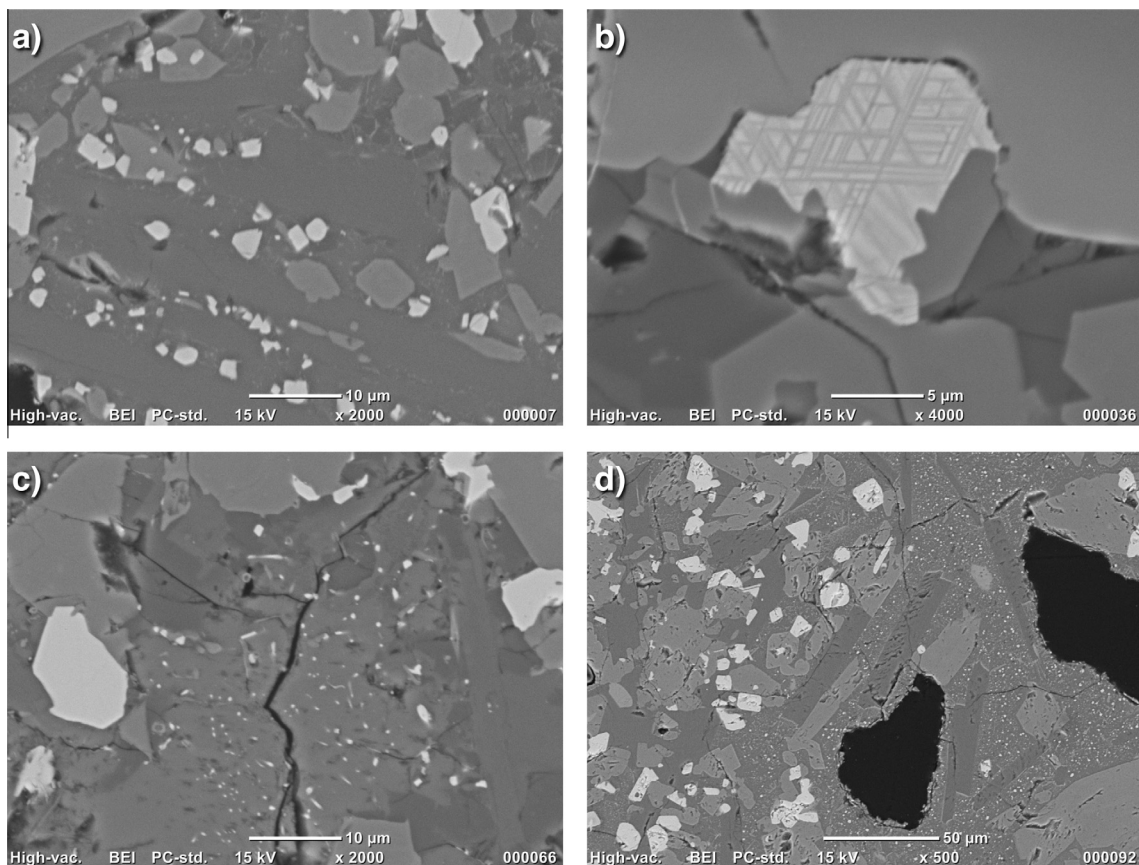

Fig. 4. Scanning electron microscope images of thin sections, showing a variety of observed behaviours. (a) Site 9 (1971, rock magnetic group H) shows small grains and no oxidation or exsolution. (b) This grain from site 1 (1949, rock magnetic group C) shows abundant ilmenite lamellae. (c) Site 6 (1646, rock magnetic group L) shows a mixture of small and larger grains, as well as dendrite-like white 'smudges'. (d) Site 11 (1949, rock magnetic group L*) reveals two distinct 'volume phases'; one with few but large magnetite grains, and one with abundant small grains.
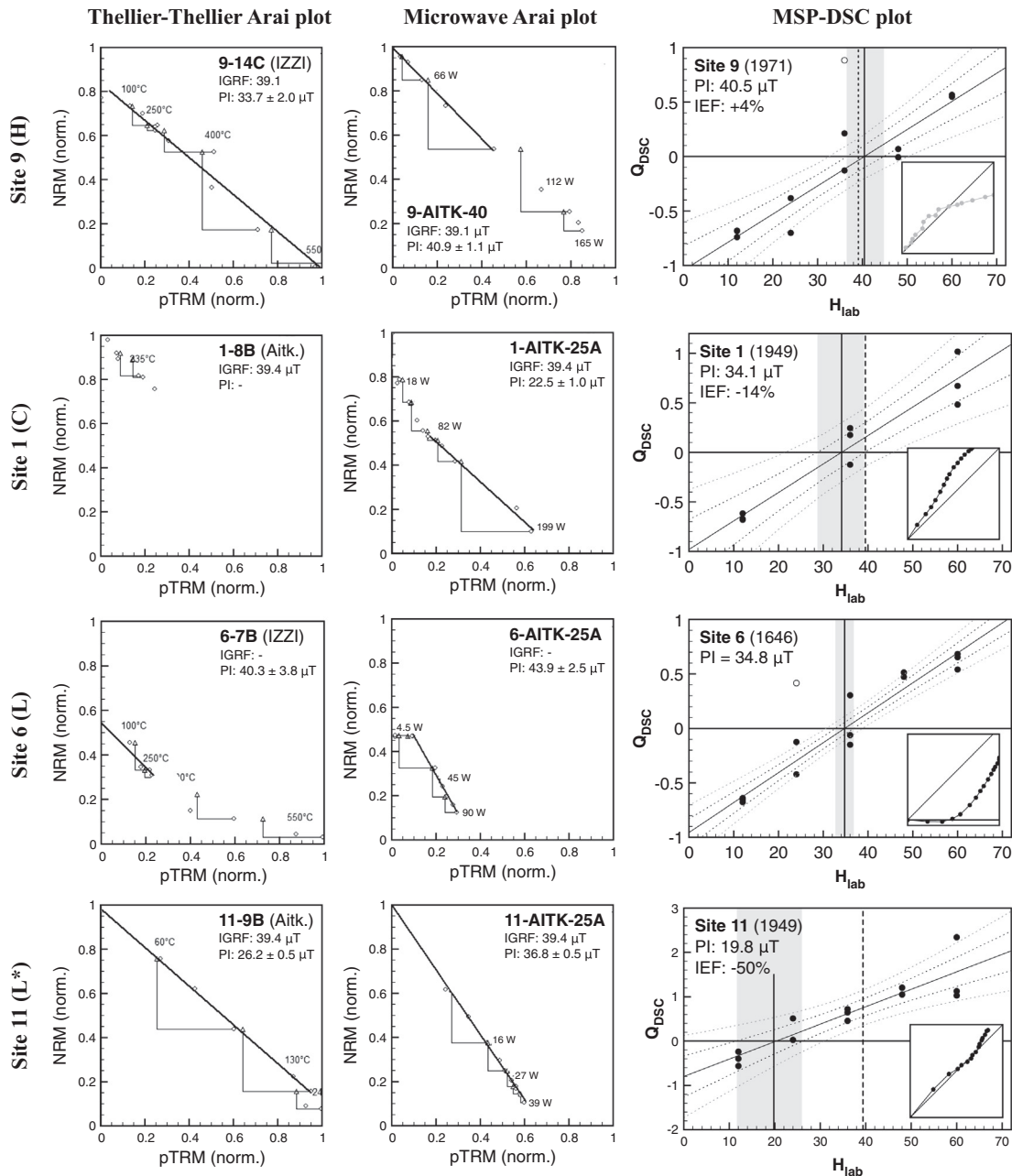
Fig. 5. Palaeointensity plots for site 9 (1971, group H), site 1 (1949, group C), site 6 (1646, group L) and site 11 (1949, group L*), the same sites as shown in Fig. 2. Both the measured palaeointensity and the IGRF value (if applicable) are shown. From left to right: Thellier–Thellier (Aitken or IZZI) Arai plot, microwave Arai plot (AITK = Aitken; numbers refer to the intensity of the laboratory field in the experiment), and multispecimen plot. Insets: schematised ARM-tests (see electronic supplement). Black and grey dotted lines are the one- and two-standard-deviation uncertainty envelopes around the lines, respectively; open dots are outlying data points excluded from the PI calculation. The grey shaded areas indicate the one-standard-deviation uncertainty envelopes in the PI estimate (black line). The vertical dashed black lines represent the IGRF value of the palaeofield (if applicable).

underestimates. Broadly speaking, it seems that sites in groups L and L* (low Curie temperatures) tend to yield large under-estimates, with the exception of site 15. Of the three high-T_c sites (groups H and C), no samples from site 1 passed the selection criteria, while site 9 yielded a palaeointensity within 10% of the expected value, and site 4 produced an overestimate. This over-estimate, however, may be explained by multi-domain effects as evidenced by the sagging visible in site 4's Arai plot (cf. Appendix 2b).

Palaeointensities obtained for the older flows seem plausible, although the values of 59.1 ± 8.3 µT for site 2 (1585) and 51.9 ± 4.0 µT for site 14 (3.2 ± 0.01 ka) seem somewhat high. In the case of site 2, this high palaeointensity may be explained by

sagging, which was also observed for sites 6 (1646) and 12 (1470–92). Site 12 yielded a low intensity value of 28.0 µT with a large standard deviation of 8.5 µT, therefore failing the criterion that the standard deviation divided by the average intensity should be less than 25%. Site 14 had the highest success rate (four out of seven) and produced the most consistent PI. Its Arai plots show straight lines up until about 400 °C degrees, after which point scatter increases. The obtained PI therefore seems reliable.

4.2.2. Microwave method

Microwave results are summarised in Table 3 and representative Arai plots are shown in Fig. 5 (middle column). All results and Arai plots can be found in Appendices 3a and 3b. The technical success

Table 3

Summary of palaeointensity results. The number of used samples n and the total number of samples, the calculated (average) PI and its standard deviation (if applicable) and the intensity error fraction (IEF; Biggin et al., 2007) are shown for all three palaeointensity methods. In the thermal Thellier experiments, three specimens per site were subjected to the Aitken protocol (six for site 4) and up to five for the IZZI protocol, depending on the amount of material left. For the MSP-DSC protocol three additional columns are added. In the ARM-test column, underest. = underestimate and overest. = overestimate, (underest.) or (overest.) signifies that the curve is close to the ideal diagonal. 'OK' indicates a successful ARM test. ε_{alt}^* is the progressive alteration (in percent) between the first and fourth heating steps (Fabian and Leonhardt, 2010). The y int. (y intercept) column shows if the linear regression passes within 10% and/or 1σ of $(0, -1)$, then labelled 'OK'. A 'OK' label between brackets indicates that the intersection was within 1σ but not within 10% of $(0, -1)$, as is often the case for sites that show substantial scatter. MSP PIs that do not pass these criteria are shown in grey. ave. = average.

	Group	Thellier–Thellier				Microwave				MSP-DSC						Ave.
		n/total	PI (μT)	σ/PI (%)	IEF (%)	n/total	PI (μT)	σ/PI (%)	IEF (%)	ARM-test	ε_{alt}^*	y int.	n/total	PI (μT)	IEF (%)	
1971 flow																
Site 4	H	5/12	46.0 ± 11.6	25%	+18%	4/9	25.1 ± 2.8	11%	−36%	OK	>3%	OK	22/28	30.1 [28.3–31.7]	−23%	**35.6 ± 14.7**
Site 8	L*	6/8	30.1 ± 6.6	22%	−23%	1/4	28.4		−27%	underest.	>3%	(OK)	14/15	24.1 [16.1–29.8]	−38%	**29.3 ± 1.2**
Site 9	H	2/6	39.8 ± 8.7	22%	+2%	6/9	41.6 ± 4.1	10%	−6%	OK?	OK	OK	11/13	39.6 [35.7–43.9]	+1%	**40.3 ± 1.1**
Combined		**13/26**	**37.7 ± 11.3**	**30%**	**−4%**	**11/22**	**34.4 ± 9.0**	**26%**	**−12%**	–	–	–	**1 site**	**39.6 [35.7–43.9]**	**+1%**	**35.8 ± 7.9**
1949 flow																
Site 1	C	0/3	–	–	–	1/5	22.5	–	−43%	underest.	OK	OK	9/9	34.1 [28.7–39.2]	−14%	**22.5**
Site 7	L*	1/8	26.6	–	−32%	1/4	42.7	–	+8%	overest.	OK	OK	14/15	49.5 [46.5–53.0]	+26%	**34.7 ± 11.4**
Site 11	L*	3/3	27.6 ± 1.4	5%	−30%	1/5	36.8	–	−7%	(underest.)	>3%	(OK)	14/14	20.3 [11.4–26.2]	−48%	**32.2 ± 6.5**
Site 13	L*	1/4	31.0	–	−21%	1/7	44.9	–	+14%	(overest.)	>3%	OK	12/13	25.3 [19.1–30.2]	−36%	**38.0 ± 9.8**
Site 15	L*	5/8	36.5 ± 3.8	10%	−7%	1/5	43.4	–	+11%	(underest.)	OK	OK	14/17	53.6 [49.2–59.6]	+36%	**40.0 ± 4.9**
Combined		**10/26**	**32.3 ± 5.3**	**16%**	**−18%**	**5/26**	**38.1 ± 9.2**	**24%**	**−3%**	–	–	–	–	–	–	**34.7 ± 8.1**
Older flows																
Site 3 (1712)	L	2/8	47.4 ± 10.3	22%	–	1/2	43.4	–	–	(overest.)	OK	OK	11/15	19.4 [...–29.7]	–	**45.4 ± 2.8**
Site 5 (1677)	L*	0/8	–	–	–	1/2	46.6	–	–	overest.	OK	(OK)	12/14	36.6 [29.0–45.2]	–	**46.6**
Site 6 (1646)	L	2/8	44.4 ± 5.7	13%	–	1/2	43.9	–	–	overest.	>3%	OK	14/15	35.0 [32.0–38.0]	–	**44.2 ± 0.4**
Site 2 (1585)	C	3/8	59.1 ± 8.3	14%	–	1/2	33.7	–	–	overest.	OK	(OK)	9/14	43.0 [39.6–47.0]	–	**46.4 ± 18.0**
Site 12 (1470–92)	L*	2/7	28.0 ± 8.5	31%	–	1/2	44.0	–	–	underest.	OK	OK	10/12	28.6 [26.3–30.8]	–	**36.0 ± 11.3**
Site 10 (1.09 ka)	H	1/4	46.7	–	–	2/3	40.5 ± 6.9	17%	–	underest.	OK	(OK)	7/8	26.7 [20.2–32.0]	–	**43.6 ± 4.4**
Site 14 (3.2 ka)	C	4/7	51.9 ± 4.0	8%	–	2/4	52.0 ± 3.1	6%	–	underest.	OK	(OK)	12/15	32.5 [28.7–36.0]	–	**52.0 ± 0.1**

rate of the microwave experiments is similar to that of the thermal Thellier experiments: 38% averaged over all sites, although it must be noted that the success rate for the five 1949 sites is drastically lower. This was mainly caused by the large amount of specimens that did not pass the initial '1 W, 0.1 s' test that was designed to test for possible changes due to the frequency sweep. However, from Table 3 it is evident that generally the microwave method produces palaeointensities that are closer to the expected intensity. Sites 9 (1971), 7 and 11 (both 1949) yielded values within 10% of the expected palaeofield, whereas sites 13 and 15 (both 1949) were within 15%. Sites 4, 8 (both 1971) and 1 (1949) yielded large underestimates, but these may be explained by sagging (sites 1 and 4) or a 'messy' Arai plot (site 8). In general, however, it seems that microwave Arai plots – at least for sites that passed the '1 W, 0.1 s' test – are more linear than their thermal Thellier counterparts.

Because of limited measuring time on the microwave system, the IGRF sites were given priority. For that reason, generally only two to three specimens per site were measured for the older sites. As many specimens failed the initial '1 W, 0.1 s' test, often only one specimen per site passed the selection criteria, making it difficult to assess their reliability. The obtained palaeointensities, however, seem plausible and compare well to model data. For the two sites (10 and 14) that produced multiple acceptable palaeointensities, microwave results were consistent.

4.2.3. Multispecimen method

A summary of MSP-DSC results is shown in Table 3 and four plots in Fig. 5. All multispecimen results (MSP-DB and MSP-DSC) can be found in Appendices 5a and 5b; results of the ARM test are shown in Appendix 4. Of the fifteen MSP experiments conducted in this study, ten showed less than 3% alteration during the experiment and are therefore considered technically successful (see Table 3). Four out of the five that failed are of rock magnetic type L or L*. In general, most sites yielded acceptable results in that their data points are on a more or less straight line and show relatively little scatter ($r^2 > 0.9$). As can be seen in Appendices 5a and 5b, the sites that showed substantial scatter in their MSP-DB plots tend to improve significantly when the DSC correction is applied. This goes in particular for sites 2 (r^2 from 0.68 to 0.95) and 9 (r^2 from 0.70 to 0.93). Looking at the eight IGRF sites it is apparent that the sites in groups H and C (4, 9 and 1) yield the most accurate results, whereas the low-T_c sites tend to dramatically overestimate (sites 7 and 15) or underestimate (sites 8, 11 and 13) the palaeofield.

Since the ARM-tests in this study were done in retrospect and on sparse sample material the quality of the ARM-tests is disappointing for some sites. Only site 4 (type H) yielded a definite positive ARM-test, but unfortunately the samples of site 4 altered more than 3% during the MSP-experiment and its results must

therefore be doubted. Indeed, the MSP-DSC plot of site 4 yields an underestimate of the palaeofield of 23%, despite its positive ARM-test (Table 3). Its MSP-DB result, however, is within 10% of the palaeofield. The ARM-test of site 9 may also be positive but is obscured by scatter among the samples; site 9 alters less than 3% during the MSP-experiment and reproduces the palaeofield within error (Fig. 5; Table 3). Both sites with a positive ARM-test are of rock magnetic type H. The ARM test correctly predicts the underestimate produced by site 1 and site 7's overestimate, but not the overestimate produced by site 15. Indeed, for sites 8, 11, 13 and 15 the ARM test is fairly close to the ideal line, whereas their obtained PIs substantially underestimate (sites 8, 11 and 13) or overestimate (site 15) the field. These sites have in common that they all have low to very low Curie temperatures. Most of them fail the alteration criterion.

5. Discussion

5.1. Rock magnetic criteria

Comparing our host of rock magnetic data to the palaeointensity results, it is apparent that sites with a low Curie temperature (groups L and L*) tend to produce the worst results (cf. the large underestimates and overestimates in Table 3 in all three methods). The microwave method often produces better results than thermal Thellier-style experiments. This may be due to the high degree of customisability of the microwave experiments, as step sizes are chosen on a per-sample basis. Interestingly, in the thermal Aitken experiments, it is the low-T_c sites that are technically the most successful, most likely because we stayed below the sites' alteration temperatures and L and L* sites tend to unblock faster, leading to a larger fraction f. High-T_c sites nearly universally failed because their fraction NRM unblocked was too small (<0.35) at these temperatures. For that reason, the IZZI-Thellier experiments were much more successful for these sites. It should be noted, however, that if a different set of selection criteria with a smaller required fraction NRM lost (e.g. $f \geqslant 0.15$ for SELCRIT2; Selkin and Tauxe, 2000) had been used, some of these samples would have passed.

A high Curie temperature, however, is not always a guarantee for success, as evidenced by for example site 14's propensity for 'messy' Arai plots (see Appendices 2b and 3b). This may be explained by the site's rather unfortunate rock magnetic characteristics. It is in the MD range (Fig. 3) and shows relatively high values of the anisotropy parameter $\%h$ and the viscosity index v (Table 1). These 'messy' plots are also observed in the other two sites (viz. 8 and 13) with high degrees of viscosity and anisotropy. It seems therefore recommendable to not only take into account a site's Curie temperature when interpreting its palaeointensity results, but also its other rock magnetic properties such as anisotropy, viscosity and the degree of oxidation. Encouragingly, site 9 (1971), the site with the most ideal rock magnetic characteristics (high T_c, close to SD, negligible oxidation and exsolution), reproduces the palaeofield to within a few per cent in all three palaeointensity methods.

5.2. Selection criteria for the Thellier–Thellier and microwave methods

The success rates for the thermal and microwave Thellier–Thellier experiments were very similar (36% and 38%, respectively). The microwave Arai plots were generally more linear than their thermal counterparts, but a fairly large number of specimens (12 out of 32 specimens within the IGRF range and several older samples) were rejected beforehand because they failed the initial '0.1 W, 1 s' test (cf. Section 3.2.2). A number of these specimens

yielded good Arai plots that were accepted by either ThellierTool A or B (class TTA and TTB, respectively). As these specimens produced inaccurate palaeointensities, sometimes up to 350% of the palaeofield, this would have significantly skewed the results. The results in class TTA do not seem significantly better than those in class TTB. Of the 10 class TTA thermal and 11 class TTA microwave specimens within the IGRF range only 1 and 4, respectively, were within 10% of the IGRF. Out of 17 class TTB thermal and 17 class TTB microwave specimens within the IGRF range, 5 and 3, respectively, were within 10% of the expected value.

A technically successful Arai plot, therefore, does not guarantee a correct estimate of the palaeofield: sites 4, 8, 7, 11 and 13 all produced large (15–32%) underestimates or overestimates in the thermal Thellier experiments, as did sites 4, 8 and 1 in the microwave experiments (cf. Table 3). In many cases, however, these plots show multi-domain behaviour (sagging) or 'messy' plots. These samples may pass the applied selection criteria for part of their Arai plot, but visual inspection would reveal them to be less than satisfactory. A combination of selection criteria and visual inspection to identify undesirable behaviour seems therefore the best option.

5.3. Multispecimen method and ARM test

The ARM test in combination with the requirement that ε_{alt} $\leqslant 3\%$ seems a good way to assess multispecimen results. For the sites for which the palaeofield is known, applying these criteria properly identified the only site that produced a correct estimate of the palaeofield. All other MSP results, which did not reproduce the palaeofields intensity correctly, were rejected. It is important to note, however, that the interpretation of the ARM test is rather subjective to date. This is to a large extent due to the limited number of sites processed so far. Only with a larger ARM test data base the interpretation of the ARM test may be quantified in the future.

Based on our results the ARM-test is only partly able to distinguish between over- and underestimates produced by the MSP-experiments that do not exhibit alteration during the experiment: for sites 1 and 7 the predictions are correct, whereas site 15 is labelled as a (small) underestimate while an overestimate is produced. Similarly, the ARM test for sites 8, 11 and 13 is close to the ideal line, but large underestimates are produced. This may be related to these sites' very low Curie temperatures. It should also be kept in mind that the technical quality of the present ARM-tests is rather disappointing since these experiments had to be done on sparingly available samples left-over after the palaeointensity study. Test results presented in de Groot et al. (2012, 2013a, 2013b) were based on a larger number of specimens and are considered more robust than those presented here.

Site 4, which yielded a positive ARM test but unfortunately showed progressive alteration ($\varepsilon_{alt} > 3\%$), did, however, reproduce the palaeofield to within 10% in the MSP-DB protocol. As the ARM test did not reveal alteration after one heating step, it may tentatively be surmised that the MSP-DB protocol – which only includes one heating step – in those cases may provide a reliable palaeointensity. The only other site that passed the ARM test, site 9, showed relatively high scatter ($r^2 = 0.70$) in its MSP-DB plot, but the obtained palaeointensity was within 10% of the expected value, further supporting this hypothesis.

5.4. Magnetic relaxation

All technically successful thermal Thellier experiments done on samples from rock magnetic type L* yield considerable (>20%) underestimates of the field, while their Arai plots are often among the most successful. For example site 11 (1949; $T_c = 80\,°C$) shows high-quality Thellier–Thellier Arai plots but yields PIs that

underestimate the palaeofield by nearly 30%. Here we explore another explanation for systematically occurring underestimates of the palaeofield: we hypothesise that for these samples with very low Curie temperatures viscous processes continue to 'mold', 'optimise', or 'cure' the NRM after the lava flow was cooled to room temperature and the initial NRM was recorded in the samples. If the NRM would be influenced by thermally activated relaxation processes, the palaeointensity experiments are anticipated to yield underestimates of the palaeofield. The moment of the original TRM is anticipated to decrease with increasing time because individual grains seek an overall lower energy configuration which is as a rule represented by a lower magnetic moment (see also De Groot et al., 2014). So, the NRM is 'too low' and when compared to a laboratory (p)TRM which did not undergo these relaxation processes, an underestimate is the result.

An experiment that may corroborate this hypothesis was a 'full-TRM experiment' on site 11 (1949). Site 11 was selected for its very low dominant Curie temperature (only 80 °C) and its systematic underestimation of the palaeofield regardless of the PI method used in this study (it should be noted, however, that the ARM-test predicted the occurrence of an underestimate). Nine specimens were heated in a field of 40 μT to a temperature of 250 °C, which is well above the site's Curie temperature of 80 °C, but well below its alteration temperature of 325 °C. Therefore, the specimens have acquired a full TRM but should have experienced negligible thermochemical alteration. However, while site 11 yielded an underestimate of 50% in the original DSC experiment with the NRM, it reproduced the laboratory field of 40 μT to within 0.5% in the full-TRM experiment (Fig. 6). This observation indeed supports our hypothesis of a viscous decay of the samples' NRM; furthermore it provides a constraint on the speed at which this magnetic relaxation occurs: it is undetectable at laboratory time scales and must therefore operate on longer time scales (i.e. days or longer).

A different hypothesis for the observed underestimates may be that the samples' NRM is a chemical remanence (CRM) or thermochemical remanence (TCRM) rather than a TRM. A CRM may result in linear Arai plots that nevertheless significantly underestimate the palaeofield (see e.g. Draeger et al., 2006). This explanation, however, seems unlikely as site 11 – like sites 8 and 13 – did not show significant oxyexsolution (cf. the SEM images in Fig. 4 and Appendix 6 in the electronic supplement of this contribution). Furthermore, none of our flows were overlain by more recent flows, thus eliminating the possibility that they were
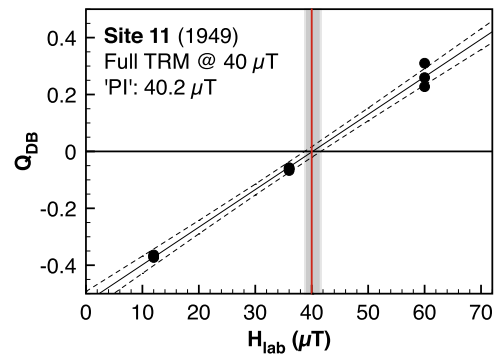

Fig. 6. Site 11 (1949, group L*). Multispecimen plot for a full-TRM induced in the laboratory in a field of 40 μT (red line). Lines and shading according to Fig. 5. The full-TRM experiment reproduces the imparted TRM of 40 μT to within 0.5%. (For interpretation of the references to colour in this figure legend, the reader is referred to the web version of this article.)

reheated by an overlying flow (e.g. baked contacts or volcanic glasses) and acquired a CRM that way (see Draeger et al., 2006).

5.5. Comparing palaeointensity methods

All palaeointensity results that pass the selection criteria applied for each method can now be compared (Fig. 7). The tendency to produce underestimates of the palaeofield for the thermal Thellier-style method is evident: of the eight IGRF sites four sites yielded large underestimates, of 21% (site 13) to 32% (site 7), while only sites 9 and 15 reproduced the palaeofield within error, and site 1 overestimated it by 18%. The intensity error fractions calculated from the microwave experiments are generally smaller and more evenly distributed between over- and underestimates. Sites 1, 4 and 8 produced large (43%, 36% and 27%, respectively) underestimates, accompanied by sagging or 'messy' plots; the other five sites reproduced the palaeofield to within 6–14%. The generally smaller IEF may be related to the smaller amount of heating experienced by the specimens in the microwave method. Specimens are subjected to lower peak temperatures for a much shorter time span than in the classic Thellier method. This should reduce both the risk of alteration as well as its extent when it does occur. The only acceptable MSP-DSC result (passed ARM test, alteration <3%) reproduces the palaeofield within error, as does the only
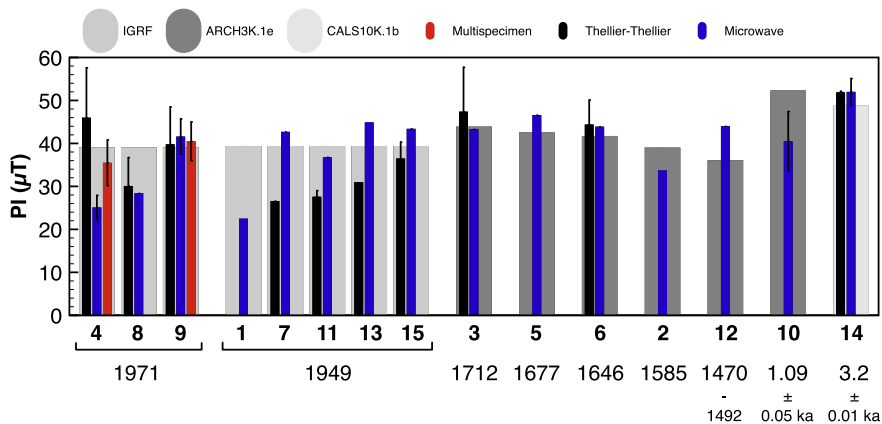

Fig. 7. Results from the three different methods per site. Only results that passed our selection criteria (ThellierTool A and B as modified by Paterson et al. (2014) for Thellier–Thellier and microwave experiments, and a positive ARM-test for the multispecimen method) are shown. Where possible for Thellier and microwave experiments, the results were averaged per site. The number of accepted results is listed in Table 3. Standard deviations are indicated by the thin black bars. If no error bar is shown, only one specimen passed the selection criteria.

accepted MSP-DB result (passed ARM test, but alteration >3%). From Fig. 7 it may be inferred that if two or three methods agree to within a few μT, the obtained palaeointensity is close to the palaeofield as was also shown by De Groot et al. (2013b). Site 9 (1971) yields palaeointensities of 39.8 ± 8.7 μT (Thellier–Thellier), 41.6 ± 4.1 μT (microwave) and 39.6 [35.7–43.9] μT (MSP-DSC), which are all within 10% of the IGRF value of 39.1 μT. Similarly, for sites 15 (1949), 6 (1646) and 14 (3.2 ± 0.01 ka) (and to a lesser extent site 3 (1712)) the Thellier–Thellier and microwave methods agree to within a few μT. The value obtained for site 15 is close to the expected IGRF intensity, whereas the older sites yield results very similar to the CALS models, which are based on palaeointensity data. Conversely, when the two Thellier-style methods yield very different palaeointensities (e.g. sites 8 (1971), 7 (1949), 11 (1949) and 13 (1949)), the obtained palaeointensities are usually more than 10% off. The only exception is site 8 (1971), whose results are consistent but significantly underestimate the palaeofield. However, while its Arai plots did pass the selection criteria, they would not pass visual inspection.

5.6. Comparing our data to models

Since our sites are at most 3.2 ka, we can compare the outcome of our experiments to descriptive models of geomagnetic field variations, such as CALS3K.1b, CALS10K.1b, and ARCH3K.1e (e.g. Korte et al., 2009, 2011), which themselves are data-driven (Fig. 8). The field models direction-wise generally appear to agree with our results (Fig. 8, upper two plots). Only site 10 (∼850 AD) shows a large deviation with a measured declination of 30° to the east while ∼10° to the west is expected and a steep measured inclination of ∼44° where ∼34° is expected. This site, however, was sampled at the edge of a small and unstable cone. Therefore it is possible that the site is not in in-situ position; movement after cooling cannot be excluded.

As scatter on the individual accepted palaeointensity results is rather large, only average values per flow per method are shown in Fig. 8. Due to differences in rock magnetic properties within one flow, the standard deviations of these averages are large (up to 30%) for the two 20th-century flows. However, the average microwave results – and for the 1971 flow also the Thellier result – reproduce the palaeofield within error. For the older flows especially the microwave results agree very well (to within a few μT) with the models. Our data therefore seem to concur with previously measured palaeointensity data and the selection procedure adopted seems robust.

If all acceptable results (e.g. Thellier and microwave classes TTA and TTB and multispecimen results that pass the ARM test and the alteration criterion and the y intersection criterion) are averaged for the two 20th-century flows the obtained palaeointensities reproduce the palaeofield to within 8% and 12%, respectively (Table 3). This implies that sampling a cooling unit at multiple locations, using various palaeointensity methods, and applying strict selection criteria indeed yields a proper estimate of the full vector of the geomagnetic field for one location and one instance in time. This concurs with the observation by Biggin et al. (2007) that if two or more materials from the same cooling unit with distinct rock magnetic properties produce palaeointensity measurements of acceptable quality, the range of values over which they overlap will very likely include the true palaeointensity.

6. Conclusions

The rock magnetic behaviour of samples has a major influence on their success rates and the outcome of various palaeointensity experiments. It is therefore important to assess this behaviour and choose the appropriate palaeointensity technique accordingly. No combination of any Thellier method applied in this study and the modified ThellierTool A and B sets of selection criteria proved capable of distinguishing between correct estimates of the
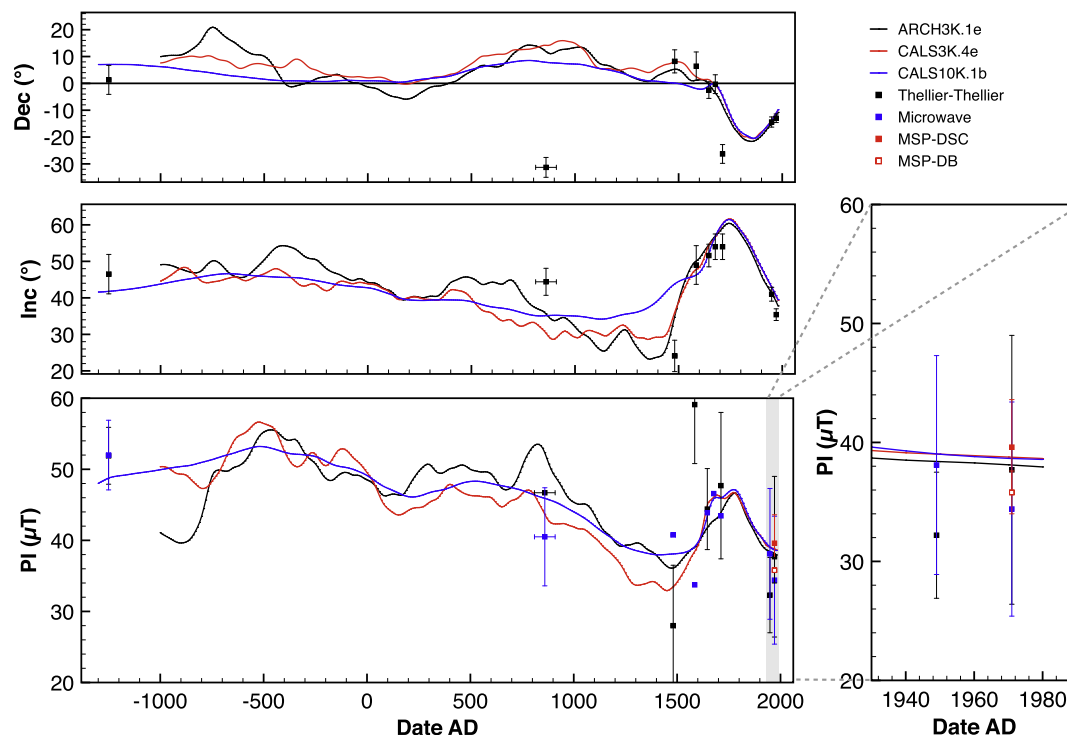

Fig. 8. Obtained declinations, inclinations and accepted palaeointensity results plotted against time and compared to the ARCH3K.1e, CALS3K.4e and CALS10.1b models (e.g. Korte et al., 2009, 2011).

palaeofield versus over- and underestimates for individual samples. Although the MSP-experiment with ARM-test and stringent alteration criterion yielded only one reliable palaeointensity estimate in this study as well as one tentative MSP-DB result, those two estimates gave the correct known field value of these historic lavas. The most reliable palaeointensities are those that are corroborated by multiple palaeointensity experiments that yield the same field estimate. Furthermore, we found indications for a viscous magnetic relaxation effect occurring in samples with very low Curie temperatures that precludes a reliable reconstruction of the palaeofield for those samples.

Acknowledgements

Appendix A. Supplementary data

Supplementary data (This supplementary information includes: rock magnetic plots for all sites (Appendix 1), Thellier–Thellier parameters and Arai plots (Appendices 2a and 2b), microwave parameters and Arai plots (Appendices 3a and 3b), ARM tests (Appendix 4), multispecimen data and plots (Appendices 5a and 5b) and SEM images (Appendix 6).) associated with this article can be found, in the online version, at http://dx.doi.org/10.1016/j.pepi.2015.03.004.

References

Aitken, M.J., Allsop, A.L., Bussell, G.D., Winter, M.B., 1988. Determination of the intensity of the Earths magnetic-field during archaeological times – reliability of the Thellier technique. Rev. Geophys. 26 (1), 3–12. http://dx.doi.org/10.1029/RG026i001p00003.

Biggin, A.J., 2006. First-order symmetry of weak-field partial thermoremanence in multi-domain (MD) ferromagnetic grains: 2. Implications for Thellier-type palaeointensity determination. Earth Planet. Sci. Lett. 245 (1–2), 454–470. http://dx.doi.org/10.1016/j.epsl.2006.02.034.

Biggin, A.J., Poidras, T., 2006. First-order symmetry of weak-field partial thermoremanence in multi-domain ferromagnetic grains. 1. Experimental evidence and physical implications. Earth Planet. Sci. Lett. 245 (1–2), 438–453. http://dx.doi.org/10.1016/j.epsl.2006.02.035.

Biggin, A.J., Perrin, M., Dekkers, M.J., 2007. A reliable absolute palaeointensity determination obtained from a non-ideal recorder. Earth Planet. Sci. Lett. 257 (3–4), 545–563. http://dx.doi.org/10.1016/j.epsl.2007.03.017.

Böhnel, H.N., Dekkers, M.J., Delgado-Argote, L.A., Gratton, M.N., 2009. Comparison between the microwave and multispecimen parallel difference pTRM palaeointensity methods. Geophys. J. Int. 177 (2), 383–394. http://dx.doi.org/10.1111/j.1365-246X.2008.04036.x.

Böhnel, H., Herrero-Bervera, E., Dekkers, M.J., 2011. Paleointensities of the Hawaii 1955 and 1960 Lava flows: further validation of the multi-specimen method. In: Petrovský, E., Ivers, D., Harinarayana, T. (Eds.), The Earth's Magnetic Interior. IAGA Special Sopron Book Series, Springer, Netherlands, pp. 195–211.

Brown, M.C., Feinberg, J. M., and Bowles, J. A., 2010. Comparison of Palaeointensity Methods using Historical Lavas from Fogo, Cape Verde (AGU abstract).

Calvo, M., Prevot, M., Perrin, M., Riisager, J., 2002. Investigating the reasons for the failure of palaeointensity experiments: a study on historical lava flows from Mt. Etna (Italy). Geophys. J. Int. 149 (1), 44–63. http://dx.doi.org/10.1046/j.1365-246X.2002.01619.x.

Carracedo, J.-C., Rodríguez-Badiola, E., Guillou, H., de Nuez, J.L., Pérez Torrado, F.J., 2001. Geology and volcanology of La Palma and El Hierro, Western Canaries. Estudios Geol.

Coe, R.S., 1967. Palaeo-intensities of the Earth's magnetic field determined from tertiary and quaternary rocks. J. Geophys. Res. 72 (1), 3247–3262. http://dx.doi.org/10.1029/JZ072i012p03247.

Day, R., Fuller, M., Schmidt, V.A., 1977. Hysteresis properties of titanomagnetites – grain-size and compositional dependence. Phys. Earth Planet. Inter. 13 (4), 260–267. http://dx.doi.org/10.1016/0031-9201(77)90108-X.

De Groot, L.V., Dekkers, M.J., Mullender, T.A.T., 2012. Exploring the potential of acquisition curves of the anhysteretic remanent magnetization as a tool to detect subtle magnetic alteration induced by heating. Phys. Earth Planet. Inter. 194, 71–84. http://dx.doi.org/10.1016/j.pepi.2012.01.006.

De Groot, L.V., Biggin, A.J., Dekkers, M.J., Langereis, C.G., Herrero-Bervera, E., 2013a. Rapid regional perturbations to the recent global geomagnetic decay revealed

by a new Hawaiian record. Nat. Commun. 4, 2727-2727. http://dx.doi.org/10.1038/ncomms3727.

De Groot, L.V., Mullender, T.A.T., Dekkers, M.J., 2013b. An evaluation of the influence of the experimental cooling rate along with other thermomagnetic effects to explain anomalously low palaeointensities obtained for historic lavas of Mt Etna (Italy). Geophys. J. Int. 193 (3), 1198–1215. http://dx.doi.org/10.1093/gji/ggt065.

De Groot, L.V., Fabian, K., Bakelaar, I.A., Dekkers, M.J., 2014. Magnetic force microscopy reveals meta-stable magnetic domain states that prevent reliable absolute palaeointensity experiments. Nat. Commun 5, 4548.

Dekkers, M.J., Böhnel, H.N., 2006. Reliable absolute palaeointensities independent of magnetic domain state. Earth Planet. Sci. Lett. 248 (1–2), 508–517. http://dx.doi.org/10.1016/j.epsl.2006.05.040.

Draeger, U., Prévot, M., Poidras, T., Riisager, J., 2006. Single-domain chemical, thermochemical and thermal remanences in a basaltic rock. Geophys. J. Int. 166 (1), 12–32. http://dx.doi.org/10.1111/j.1365-246X.2006.02862.x.

Dunlop, D.J., 2002. Theory and application of the day plot (Mrs/Msversus Hcr/Hc) 1. Theoretical curves and tests using titanomagnetite data. J. Geophys. Res. Solid Earth 107 (B3), 2056. http://dx.doi.org/10.1029/2001JB000486.

Fabian, K., 2001. A theoretical treatment of palaeointensity determination experiments on rocks containing pseudo-single or multi domain magnetic particles. Earth Planet. Sci. Lett. 188 (1–2), 45–58.

Fabian, K., Leonhardt, R., 2010. Multiple-specimen absolute palaeointensity determination: an optimal protocol including pTRM normalization, domain-state correction, and alteration test. Earth Planet. Sci. Lett. 297 (1), 84–94. http://dx.doi.org/10.1016/j.epsl.2010.06.006.

Fanjat, G., Camps, P., Shcherbakov, V., Barou, F., Sougrati, M.T., Perrin, M., 2012. Magnetic interactions at the origin of abnormal magnetic fabrics in lava flows: a case study from Kerguelen flood basalts. Geophys. J. Int. 189, 815–832.

Herrero-Bervera, E., Valet, J.P., 2009. Testing determinations of absolute paleointensity from the 1955 and 1960 Hawaiian flows. Earth Planet. Sci. Lett. 287, 420–433.

Hill, M.J., Shaw, J., 1999. Palaeointensity results for historic lavas from Mt Etna using microwave demagnetization/remagnetization in a modified Thellier-type experiment. Geophys. J. Int. 139 (2), 583–590.

Klugel, A., Schmincke, H.U., White, J., Hoernle, K.A., 1999. Chronology and volcanology of the 1949 multi-vent rift-zone eruption on La Palma (Canary Islands). J. Volcanol. Geoth. Res. 94, 267–282.

Korte, M., Donadini, F., Constable, C.G., 2009. Geomagnetic field for 0–3 ka: 2. A new series of time-varying global models. Geochem. Geophys. Geosyst. 10 (6). http://dx.doi.org/10.1029/2008GC002297.

Korte, M., Constable, C., Donadini, F., Holme, R., 2011. Reconstructing the Holocene geomagnetic field. Earth Planet. Sci. Lett. 312 (3–4), 497–505. http://dx.doi.org/10.1016/j.epsl.2011.10.031.

Krása, D., Heunemann, C., Leonhardt, R., Petersen, N., 2003. Experimental procedure to detect multidomain remanence during Thellier–Thellier experiments. Phys. Chem. Earth Parts A/B/C 28 (16–19), 681–687. http://dx.doi.org/10.1016/S1474-7065(03)00122-0.

Leonhardt, R., Heunemann, C., Krása, D., 2004a. Analyzing absolute palaeointensity determinations: acceptance criteria and the software ThellierTool4.0. Geochem. Geophys. Geosyst. 5 (12). http://dx.doi.org/10.1029/2004GC000807.

Leonhardt, R., Krása, D., Coe, R.S., 2004b. Multidomain behavior during Thellier palaeointensity experiments: a phenomenological model. Phys. Earth Planet. Inter. 147 (2–3), 127–140. http://dx.doi.org/10.1016/j.pepi.2004.01.009.

Mullender, T., van Velzen, A.J., Dekkers, M.J., 1993. Continuous drift correction and separate identification of ferrimagnetic and paramagnetic contributions in thermomagnetic runs. Geophys. J. Int. 114 (3), 663–672. http://dx.doi.org/10.1111/j.1365-246X.1993.tb06995.x.

Paterson, G.A., Tauxe, L., Biggin, A.J., Shaar, R., Jonestrask, L.C., 2014. On improving the selection of Thellier-type paleointensity data. Geochem. Geophys. Geosyst. http://dx.doi.org/10.1002/2013GC005135.

Riisager, P., Riisager, J., 2001. Detecting multidomain magnetic grains in Thellier palaeointensity experiments. Phys. Earth Planet. Inter. 125 (1), 111–117. http://dx.doi.org/10.1016/S0031-9201(01)00236-9.

Selkin, P.A., Tauxe, L., 2000. Long-term variations in palaeointensity. Philos. Trans. Math. Phys. Eng. Sci. 358 (1768), 1065–1088.

Soler, V., Carracedo, J.C., Heller, F., 1984. Geomagnetic secular variation in historical lavas from the Canary-Islands. Geophys. J. Roy. Astron. Soc. 78 (1), 313–318. http://dx.doi.org/10.1111/j.1365-246X.1984.tb06487.x.

Tauxe, L., Constable, C., Stokking, L., Badgley, C., 1990. Use of anisotropy to determine the origin of characteristic remanence in the Siwalik red beds of Northern Pakistan. J. Geophys. Res. Solid Earth Planets 95, 4391–4404.

Thellier, E., Thellier, O., 1959. Sur l'intensité du champ magnétique terrestre dans le passé historique et géologique. Ann. Geophys.

Valet, J., Soler, V., 1999. Magnetic anomalies of lava fields in the Canary Islands. Possible consequences for palaeomagnetic records. Phys. Earth Planet. Inter. 115 (2), 109–118.

Watkins, N.D., Haggerty, S.E., 1968. Oxidation and magnetic polarity in single Icelandic Lavas and dikes. Geophys. J. Int. 15, 305–315.

Yamamoto, Y., Tsunakawa, H., Shibuya, H., 2003. Palaeointensity study of the Hawaiian 1960 lava flow: implications for possible causes of erroneously high intensities. Geophys. J. Int. 153, 263–276.

Yu, Y.J., Tauxe, L., Genevey, A., 2004. Toward an optimal geomagnetic field intensity determination technique. Geochem. Geophys. Geosyst. 5 (2). http://dx.doi.org/10.1029/2003GC000630.

Yu, Y.J., Tauxe, L., 2005. Testing the IZZI protocol of geomagnetic field intensity determination. Geochem. Geophys. Geosyst. 6 (5). http://dx.doi.org/10.1029/2004GC000840.